Heteroepitaxial growth of β-Ga_2O_3 thin films on single crystalline diamond (111) substrates by radio frequency magnetron sputtering

Kusaba, Takafumi
Department of Advanced Energy Science and Engineering, Kyushu University

Sittimart, Phongsaphak
Department of Advanced Energy Science and Engineering, Kyushu University

Katamune, Yuki
Department of Electrical and Electronic Engineering, Kyushu Institute of Technology

Kageura, Taisuke
Sensing System Research Center, National Institute of Advanced Industrial Science and Technology (AIST)

他

https://hdl.handle.net/2324/7183508

出版情報：Applied Physics Express. 16 (10), pp.105503-, 2023-10-09. IOP Publishing
バージョン：

Applied Physics Express

Heteroepitaxial growth of β-Ga_2O_3 thin films on single crystalline diamond (111) substrates by radio frequency magnetron sputtering

To cite this article: Takafumi Kusaba *et al* 2023 *Appl. Phys. Express* **16** 105503

OPEN ACCESS

Applied Physics Express **16**, 105503 (2023)

LETTER

https://doi.org/10.35848/1882-0786/acfd07

Heteroepitaxial growth of β-Ga_2O_3 thin films on single crystalline diamond (111) substrates by radio frequency magnetron sputtering

Takafumi Kusaba[1], Phongsaphak Sittimart[1,2*], Yuki Katamune[3], Taisuke Kageura[2], Hiroshi Naragino[1], Shinya Ohmagari[2], Sreenath Mylo Valappil[1], Satoki Nagano[1], Abdelrahman Zkria[4,5], and Tsuyoshi Yoshitake[1*]

[1] *Department of Advanced Energy Science and Engineering, Kyushu University, 6-1 Kasuga-koen, Kasuga, Fukuoka 816-8580, Japan*
[2] *Sensing System Research Center, National Institute of Advanced Industrial Science and Technology (AIST), 807-1 Shuku-machi, Tosu, Saga 841-0052, Japan*
[3] *Department of Electrical and Electronic Engineering, Kyushu Institute of Technology, 1-1 Sensuicho, Tobata, Kitakyushu, Fukuoka 804-8550, Japan*
[4] *Department of Physics, Faculty of Science, Aswan University, Aswan 81528, Egypt*
[5] *Center for Japan-Egypt Cooperation in Science and Technology (E-JUST Center), 6-1 Kasuga-koen, Kasuga, Fukuoka 816-8580, Japan*

*E-mail: phongsaphak_sittimart@kyudai.jp; tsuyoshi_yoshitake@kyudai.jp

Received August 9, 2023; revised September 19, 2023; accepted September 25, 2023; published online October 9, 2023

In this work, we demonstrate the first achievement in heteroepitaxial growth of β-Ga_2O_3 thin films on single crystalline diamond (111) wafers using RF magnetron sputtering. A single monoclinic (β-phase) structure with a monofamily $\{\bar{2}01\}$ plane was obtained. XRD pole figure shows $(\bar{2}02)$ and (002) textures of the $(\bar{2}01)$ β-Ga_2O_3 plane parallel to (111) diamond with six distinct rotational domains, confirming successful epitaxial growth. Collectively, this research provides valuable insights into the epitaxial growth of β-Ga_2O_3 on diamond via sputtering, paving the way for scalable β-Ga_2O_3/diamond heterostructures for future electronic and optoelectronic applications with not only high performance but also effective self-thermal management. © 2023 The Author(s). Published on behalf of The Japan Society of Applied Physics by IOP Publishing Ltd

Supplementary material for this article is available online

So far, wide bandgap semiconducting beta-gallium oxide (β-Ga_2O_3) has been the focus of much research for its potential use in future electronic devices that can operate under extreme conditions.[1–4] This is because of its exceptional physical properties, including a wide bandgap of 4.5–4.9 eV, high breakdown field (~8 MV cm^{-1}), resistance to chemical damage, and ability to withstand high levels of radiation and thermal stress.[5,6] Additionally, the cost of producing a single crystalline wafer of β-Ga_2O_3 is lower than that of producing SiC and GaN wafers, making it a more commercially viable option.[7] Despite its many advantages, power electronic devices using β-Ga_2O_3 face a self-heating problem when operating in high-power transmission circuits due to the material low thermal conductivity, which ranges from 10–30 W m^{-1} K^{-1}.[8] To overcome this problem, it is expected that an optimal electronic device would use β-Ga_2O_3 in combination with another material with a high thermal conductivity as a heat spreader. Among wide bandgap semiconductors, diamond is considered to be the most suitable material for such electronic devices. This is in regard to its exceptional physical properties, including its extremely high thermal conductivity of approximately 2000 W m^{-1} K^{-1}, high mobilities for both electrons and holes (4500 and 3800 cm^2 V^{-1} s^{-1}, respectively), high breakdown field of approximately 10 MV cm^{-1}, and resistance to harsh environmental conditions such as high temperature and strong radiation.[9–12] In addition, the doping type of diamond, especially p-type B-doped diamond, can be precisely controlled, which is the opposite of the case with β-Ga_2O_3 (natural n-type conduction). As above-mentioned, the promising combination of β-Ga_2O_3 and diamond, in which diamond can be used as either an active layer or a heat spreader for use in optoelectronic and electronic devices, has become a popular research topic.

Several techniques have been employed to form a heterostructure consisting of a β-Ga_2O_3 thin layer and a single crystalline diamond (SCD) wafer.[6,13–16] The van der Waals interactive forces technique has recently been widely employed to form the Ga_2O_3/diamond heterostructure. However, the cleavage occurring along the β-Ga_2O_3 (001) plane obstructs the ability to form a substantial and uninterrupted layer of β-Ga_2O_3 on the diamond. A different approach has been demonstrated with a β-Ga_2O_3/diamond heterostructure fabricated using a direct-bonding technique. Even this approach could provide a larger area and almost uninterrupted β-Ga_2O_3 layer bonded to the diamond wafer.[13] The edge of the bonded area experienced distortion of the lattice structures, which may degrade the adhesion of the interfacial bonds between the thin exfoliated β-Ga_2O_3 layer and the diamond wafer when the heterostructure is practically applied at high temperature. A feasible approach to achieve a scalable heterostructure of β-Ga_2O_3 on diamond is through heteroepitaxial growth. To date, the integration of Ga_2O_3 and diamond using such direct growth has not been documented. This is, therefore, a challenge to fabricate a scaled-up heterostructure of β-Ga_2O_3 and diamond by direct growth. The magnetron sputtering technique has been widely used for various film preparations and is readily accessible for industrial applications. Several advantages of this technique, such as low-pressure sputtering achieved by effectively confining plasma species using electric and magnetic fields at the front of the magnetron cathode, high plasma density, ability of large area deposition, high purity of the deposited films due to low-pressure deposition and high kinetic energy of species arriving at the substrate,[17–19] expectedly facilitate the epitaxial growth of β-Ga_2O_3 thin films on a diamond wafer. Moreover, the achievement of direct growth between β-Ga_2O_3 thin films and diamonds, and vice versa, has been hidden so far. In this work, the achievement of epitaxial growth of β-Ga_2O_3 thin films on single crystalline diamond wafers via sputtering technique is demonstrated. Monofamily crystal $\{\bar{2}01\}$ plane of the β-Ga_2O_3 thin films grown on the diamond was achieved by optimizing the substrate temperature. The epitaxial formation of β-Ga_2O_3 thin films on the diamond was confirmed using X-ray diffraction (XRD) pole-figure (PF) analysis. Based on the structural analysis, the estimation of the lattice mismatch between the β-Ga_2O_3 thin films and single crystalline diamond is revealed and discussed in detail.

β-Ga_2O_3 thin films were epitaxially grown on SCD substrates by RF magnetron sputtering (RFMS). A commercially undoped-Ga_2O_3 target with a purity of 4N and Ib-type (111) SCD (Sumitomo Corp., Japan) with dimensions of $2 \times 2 \times 0.3$ mm^3 and an off-oriented angle of $1° \sim 3°$ were used as the material target and substrates, respectively. Prior to film growth, the SCD substrates were ultrasonically cleaned with acetone, methanol, and DI water for 5, 5, and 10 min, respectively. Then, the cleaned substrate was introduced into a sputtering chamber with a based pressure of $\sim$1–4 $\times 10^{-6}$ Pa. By using a metal mask, β-Ga_2O_3 thin films with circular shapes were grown on the SCD substrates at different substrate temperatures of 400, 500, 600, and 700 °C. During the growth of β-Ga_2O_3 thin films, the growth pressure was kept at 1.5×10^{-1} Pa by stabilizing the Ar gas flow rate at 15 sccm, which the low pressure is expected to promote epitaxial formation between β-Ga_2O_3 and diamond. Note that the β-Ga_2O_3 films were grown without an O_2 gas supply. The sputtering power and deposition time were fixed at 50 W and 48 h, respectively. Figure 1(a) shows a structural drawing of the β-Ga_2O_3 thin films epitaxially grown on SCD (111) substrates using RFMS. The right upper side inset of Fig. 1(a) illustrates an expected atomic bonding between the oxygen atoms of Ga_2O_3 and the carbon atoms of a diamond at the interface of the Ga_2O_3/diamond heterostructure, the C–O bond may improve the adhesion between the grown Ga_2O_3 thin films and the diamond substrates. The thickness of the grown samples was measured using a surface profiler (Alpha-Step IQ). The structural investigation was performed by the XRD technique (SmartLab X-ray diffractometer, Rigaku Corp., Japan), and the epitaxial formation of the grown β-Ga_2O_3 thin film and SCD was confirmed by PF XRD analysis. In addition, the chemical stoichiometry of the grown films was characterized by X-ray photoelectron spectroscopy (XPS; Kratos Analytical, Shimadzu Group Corp., Japan).

The relationship between film thickness and substrate temperatures for β-Ga_2O_3 thin films grown on diamond (111) substrates is shown in Fig. 1(b). The thickness of the films grown at the substrate temperature of 400, 500, 600 and 700 °C were 1460, 1251, 823, and 315 nm, respectively. As the same growth condition with different substrate temperatures, the growth rate of the β-Ga_2O_3 films by sputtering significantly depended on the growth temperature, which was relatively low at 700 °C (0.11 nm min^{-1}). A possible reason is a re-evaporation phenomenon of adatoms on the diamond surface under the higher substrate temperature. However, this low growth rate should promote the epitaxial formation between β-Ga_2O_3 and diamond due to the longer time of adatom diffusion on terraces. The XRD patterns of the Ga_2O_3 films grown on SCD (111) substrates at different substrate temperatures of 400, 500, 600 and 700 °C are shown in Figs. 1(c) and 1(d). According to the $2\theta-\theta$ scan mode pattern, no diffraction peaks of the films grown at 400 °C are observed, indicating the formation of amorphous Ga_2O_3. Small peaks at 2θ of 30.1° and 64.9°, which possibly are due to (400) and (512) crystalline planes of monoclinic structure (β-phase) or (220) and (440) crystalline planes of spinel structure (γ-phase) in sequence,[20] are found in the films grown at 500 °C, suggesting the formation of a mixed β/γ-Ga_2O_3 structure, which is polymorphically confirmed by the appearance of multiple diffraction peaks in 2θ scan mode pattern as shown in Fig. 1(d). Under substrate temperatures above 600 °C, this mixed β/γ-Ga_2O_3 structure is recrystallized to be only β phase structure with a single family $\{\bar{2}01\}$ plane, including $(\bar{2}01)$, $(\bar{4}02)$ and $(\bar{6}03)$ at 2θ of 18.94°, 38.44° and 59.18°, respectively. It is important to note that the incident angle of XRD 2θ scan mode was fixed at 0.5° for the measurement of all samples. The $\{\bar{2}01\}$ family planes are probably formed parallel with the (111) plane of the SCD substrate. The results suggest that the single crystal (β) phase of Ga_2O_3 thin films grown on SCD (111) substrates by RFMS can be grown at substrate temperatures above 600 °C. Nevertheless, multi-crystal orientational planes, including β(400), β(111), $\beta(\bar{4}02)$, β(311), and β(512), of the β-Ga_2O_3 thin film grown at 600 °C are observed in the 2θ scan mode pattern shown in Fig. 1(d), indicating the textured polycrystalline structure of β-Ga_2O_3. In contrast to the β-Ga_2O_3 thin films grown at 600 °C, not only the single $\{\bar{2}01\}$ family planes in the $2\theta-\theta$ scan mode pattern but also no diffraction peaks in the 2θ scan mode pattern are observed in the case of the β-Ga_2O_3 thin film grown at 700 °C, implying that the $(\bar{2}01)$-oriented β-Ga_2O_3 thin film is highly feasible to be formed on SCD (111) substrates. Figure 1(e) shows rocking curves concerning the $(\bar{2}01)$ peaks of β-Ga_2O_3 thin films grown at substrate temperatures of 600 and 700 °C. The FWHM values are 4.1° and 3.0° at 600 and 700 °C, respectively. The decrease in FWHM with increasing substrate temperature indicates the improvement of crystallinity with increasing substrate temperature. The higher substrate temperature promotes the β-phase crystallization of Ga_2O_3 and reduces the diamond surface energy, which stimulates the mobility of adatoms to migrate on the diamond terraces, improving the capability of the layer-by-layer growth process. It is important to note that the β-Ga_2O_3 thin films of this work are grown by sputtering under relatively low growth pressure (1×10^{-1} Pa). The low growth pressure is also expected to increase the kinetic energy of sputtered species due to the increased mean free path, which should be effective for growth at low temperatures.

To further investigate the formation between the β-Ga_2O_3 thin films and the diamond substrates, the fabricated samples were measured using the XRD PF technique with a fixed 2θ of 91.51° for diamond and 31.76° for β-Ga_2O_3, as the results presented in Fig. 2(a). For the diamond (111) substrate, each sample was individually checked for crystallinity and crystal orientation of the substrate before the measurement of the grown β-Ga_2O_3 films. The PF of the diamond (111) substrate used in the sample fabricated at 700 °C shows 3-fold symmetric spots around $\psi = 59.2° \pm 4°$, which are rotationally separated from each other by $\phi = 120° \pm 4°$. These variants correspond to {113} crystal plane of diamond (111) stereographic projection. This result confirms the single crystallinity of diamond (111) substrate with a highly oriented crystal plane. For the grown β-Ga_2O_3, 6-fold symmetric spot groups

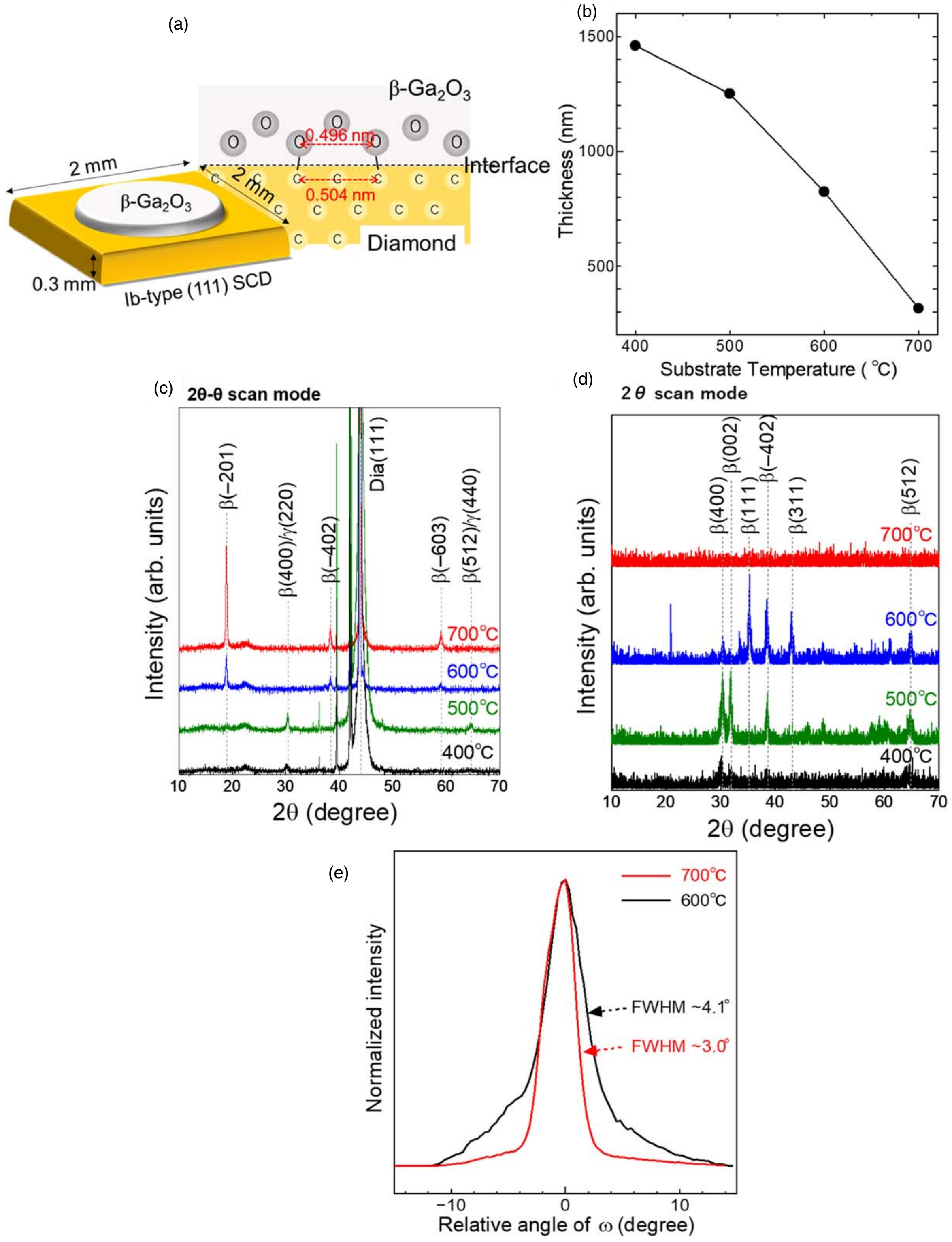

Fig. 1. (a) Structural drawing of β-Ga$_2$O$_3$ thin films grown on SCD (111) substrate by RF sputtering and right upper inset illustrating an expected atomic bond between the oxygen atom of Ga$_2$O$_3$ and the carbon atoms of diamond at the interface of the Ga$_2$O$_3$/diamond heterostructure. (b) Relationship between film thickness and substrate temperature for β-Ga$_2$O$_3$ thin films grown on diamond (111) substrates. XRD patterns of the grown β-Ga$_2$O$_3$ thin films measured in (c) $2\theta-\theta$ scan and (d) 2θ scan modes. (e) XRD rocking curves of β-Ga$_2$O$_3$ ($\bar{2}01$) peak for the samples grown at 600 and 700 °C.

are observed around $\psi = 22°$ and 50° for β-Ga$_2$O$_3$ thin films grown at the substrate temperature of 700 °C. These pole spot groups are identified as β-Ga$_2$O$_3$($\bar{2}02$) at $\psi = 22°$ and β-Ga$_2$O$_3$(002) at $\psi = 50°$, which are in good agreement with the calculated ψ values assuming a perfect β-Ga$_2$O$_3$ structure ($\psi = 22.50°$ for β-Ga$_2$O$_3$($\bar{2}02$) and $\psi = 49.92°$ for β-Ga$_2$O$_3$(002)).[21] The pole spots are rotationally separated from each other by $\phi = 60° \pm 1°$. These two distinct textures were also found in the epitaxial growth of β-Ga$_2$O$_3$ ($\bar{2}01$) on (110) and (0001) sapphires.[21–23] This indicates that the β-Ga$_2$O$_3$ thin films with the ($\bar{2}01$) preferred orientation are grown not only in the perpendicular direction but also parallel to the diamond (111) substrate with six distinct in-plane rotation domains, namely the heteroepitaxial growth of the

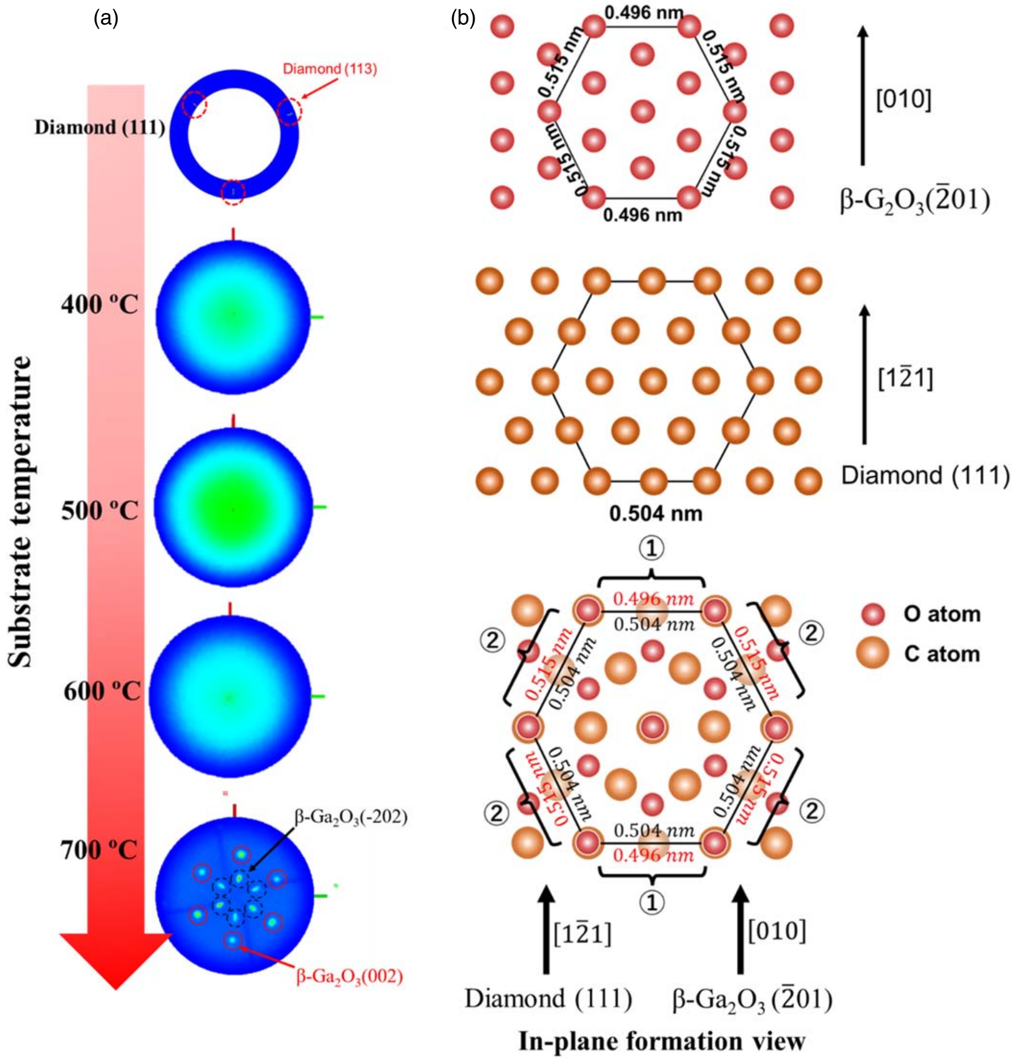

Fig. 2. (a) XRD PFs of β-Ga_2O_3 thin films grown on SCD (111) substrates with different substrate temperatures, measured at a fixed 2θ of 31.76° and (b) drawing of in-plane formation between β-Ga_2O_3 $(\bar{2}01)$ and diamond (111).

β-Ga_2O_3 thin films on diamond (111). The similarity of in-plane atomic arrangement between oxygen atoms of the β-Ga_2O_3 $(\bar{2}01)$ and carbon atoms of the diamond (111) is believed to facilitate this heteroepitaxial formation. Figure 2(b) shows the in-plane atomic arrangement between oxygen on β-Ga_2O_3 $(\bar{2}01)$ in [010] direction and carbon on diamond (111) in $[1\bar{2}1]$ direction. On the one hand, the carbon atom arrangement on the diamond (111) is a symmetric hexagonal shape with a side distance of 0.504 nm, on the other hand, the oxygen atom arrangement on the β-Ga_2O_3 $(\bar{2}01)$ is an asymmetric hexagonal shape with two different side distances of 0.496 nm and 0.515 nm, resulting in an appearance of two kinds of oxygen atom positions in which two oxygen atoms in each side located on top of the carbon atoms and the rest of the oxygen atoms located between three carbon atoms as depicted in Figs. 1(a) and 2(b) in right-bottom side. The lattice mismatch between the diamond (111) and β-Ga_2O_3 $(\bar{2}01)$ planes was calculated to be approximately −1.584 to 2.183%, which is comparable to that of C-plane sapphire (1.7% ~ 4.8%),[22] which is often used as a substrate for heteroepitaxial growth of β-Ga_2O_3 films.

Figure 3 shows surface SEM images of β-Ga_2O_3 thin films grown on SCD (111) substrates at different substrate temperatures. The surface of the film grown at 400 °C substrate temperature consists of innumerable nanocrystallites, as shown in Fig. 3(a). An increase in the grain size on the surface of the thin film with increasing substrate temperature is observed, wherein large and randomly oriented grains can be seen in the film grown at 600 °C. This polymorphic texture is consistent with the 2θ scan mode pattern result. Surprisingly, flat regions interspersed with mountain-liked crystals are observed on the surface of the film grown at 700 °C, as shown in Fig. 3(d). These surface structures may indicate that β-Ga_2O_3 thin films were grown on SCD (111) substrates by the Stranski–Krastanov (S–K) growth mode, in which the two-dimensional (2D) mode occurs in the early stages of growth and then it changes to three-dimensional (3D) island growth when the critical thickness of the grown film is exceeded.[24] Optimization of the film thickness is required to further flatten the surface of β-Ga_2O_3 thin films grown on SCD (111).

Figure 4(a) shows XPS survey spectra of the β-Ga_2O_3 thin films prepared on diamond (111) substrates at substrate temperatures of 400, 500, 600, and 700 °C. The survey spectra of all samples reveal distinct peaks corresponding to Ga 3d, O 1s, and C 1s photoelectrons. In particular, the observed C 1 s peaks in

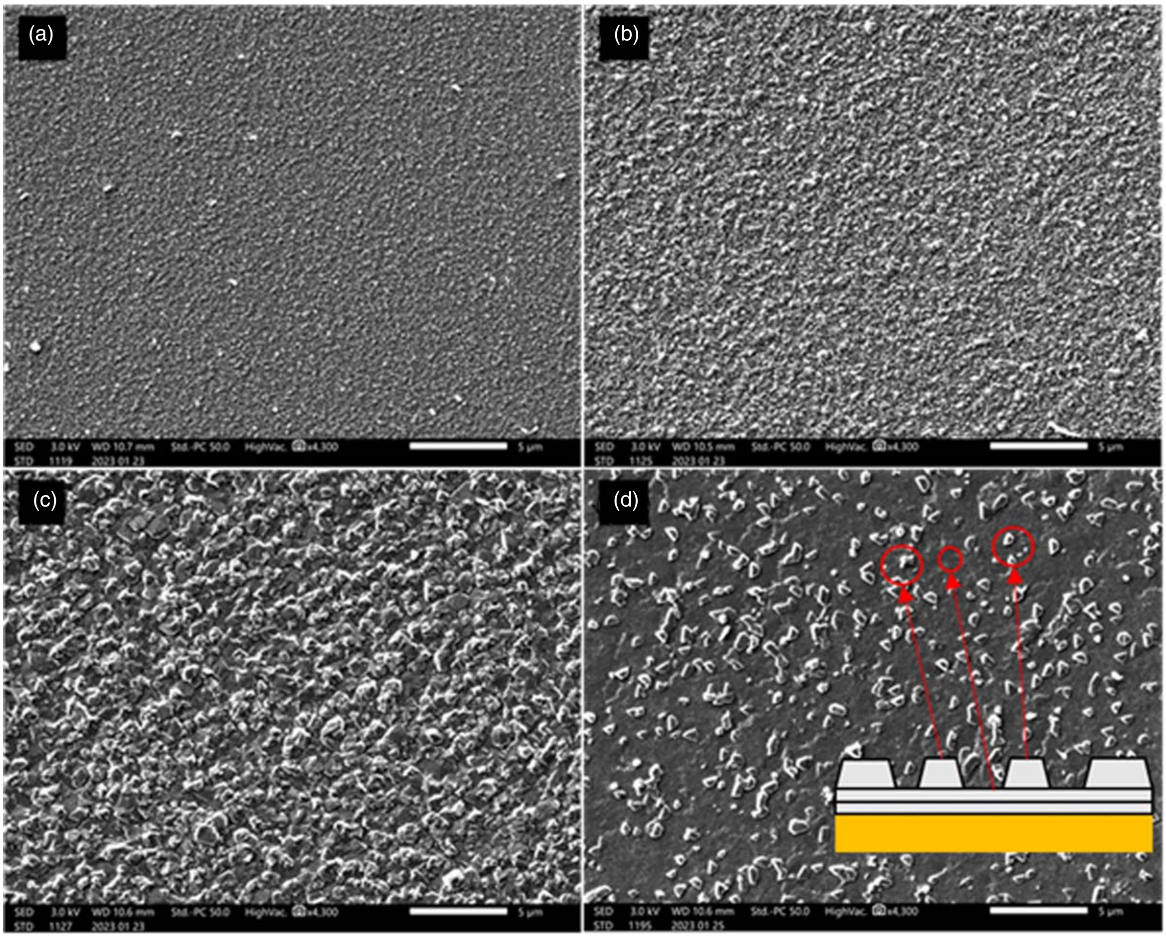

Fig. 3. Top-view SEM images of β-Ga_2O_3 thin films grown on SCD (111) substrates under different substrate temperatures of (a) 400, (b) 500, (c) 600, and (d) 700 °C. Inset of (d) is a drawing of film structure grown under S–K mode.

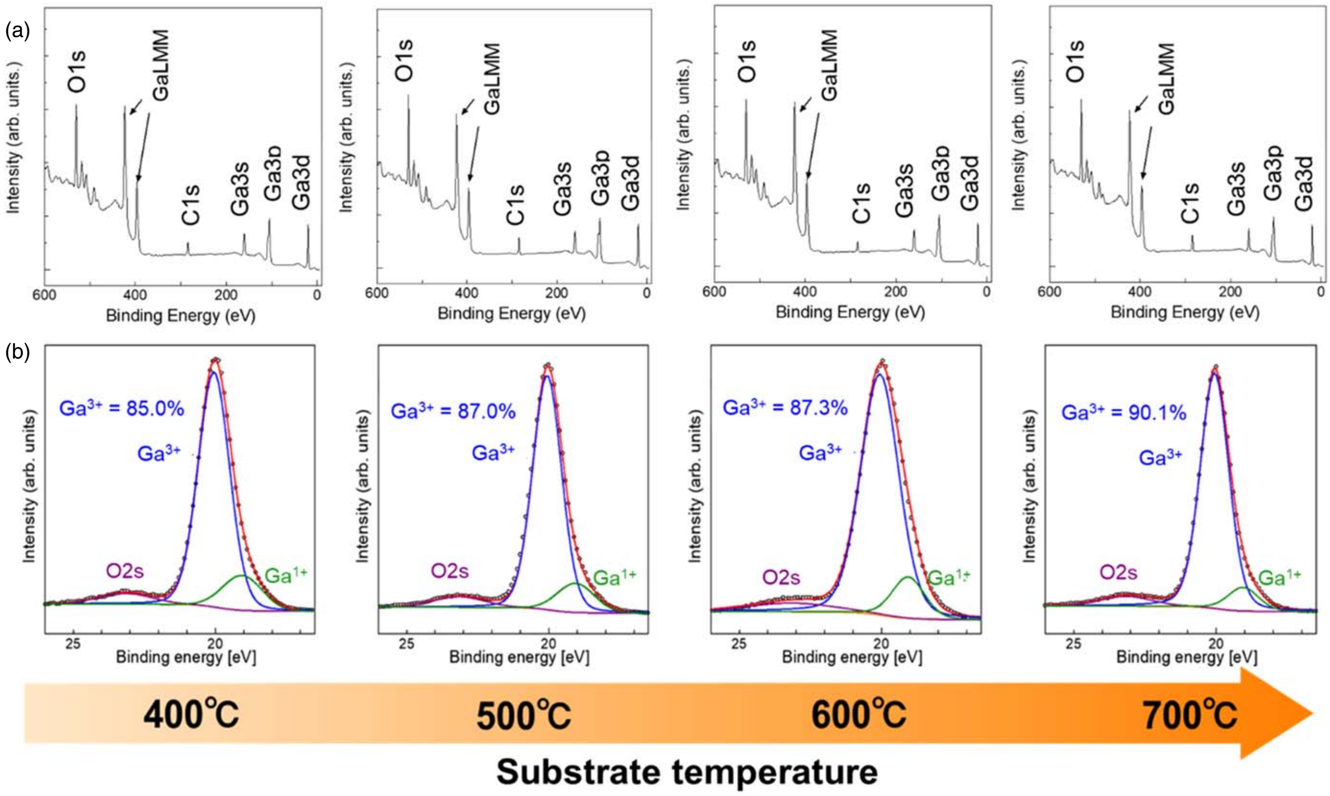

Fig. 4. (a) XPS survey spectra of β-Ga_2O_3 thin films on diamond (111) substrates prepared at various substrate temperatures and (b) peak separation of XPS Ga 3d spectrum.

Table I. Ga-O atomic ratio of β-Ga_2O_3 thin films on diamond (111) substrates, extracted from XPS spectra.

Substrate temperature	Ga[at%]	O[at%]	Ga:O
400 °C	47.56	54.44	1:1.14
500 °C	47.87	52.13	1:1.10
600 °C	46.23	53.77	1:1.16
700 °C	43.31	56.69	1:1.31
Ideally atomic composition	40	60	1:1.5 (2:3)

the spectra are likely due to the adsorption of adventitious carbon impurities on the surface, which can be terminated by heat treatment. The standard binding energy of C 1S centered at 284.8 eV was used to calibrate the peak position of other elements.[25] It is necessary to point out that the grown β-Ga_2O_3 thin films in this work were not modified by any post-treatment processes. To estimate the atomic composition of the grown films, a narrow XPS scan of the Ga 3d position was performed in the binding energy range of 16–26 eV. Figure 4(b) shows the peak-separated Ga 3d spectra of the β-Ga_2O_3 thin films grown at different substrate temperatures. The Ga 3d peak could be separated into two peaks centered at 20.06 eV and 19.06 eV, corresponding to Ga^{3+} (Ga_2O_3) and Ga^{1+} (Ga_2O, oxygen deficiency),[26,27] respectively. The oxidation state was calculated by $Ga^{3+}/(Ga^{3+}+Ga^{1+})$, which could implicitly indicate the ratio between Ga_2O_3 and Ga_2O in the grown β-Ga_2O_3 thin films. As an estimation, the Ga^{3+} peak area ratio increases with increasing substrate temperature. The largest Ga^{3+} peak area ratio of 90.1% was found in the films grown at 700 °C, indicating the abundant existence of Ga_2O_3. Table I shows the atomic composition ratios of Ga and O extracted from the O 1 s and Ga 3d spectra. As the calculation, the Ga:O ratio of the grown films is gradually brought near the ideal composition with increasing substrate temperature. The composition ratio of Ga:O = 1:1.31 was obtained for β-Ga_2O_3 thin films grown at 700 °C, which is the closest to that of perfect β-Ga_2O_3 atomic composition (Ga:O = 1:1.5). The absence of oxygen atoms presumably implies the existence of oxygen vacancies (VO) in the β-Ga_2O_3 structure which is a typical point-defect in wide bandgap semiconducting β-Ga_2O_3 thin films.[28,29] Overall, these XPS results suggested that a high substrate temperature deposition by sputtering is effective in suppressing the generation of oxygen defects and an acceptable atomic composition of β-Ga_2O_3 thin films grown on SCD (111) substrates could be achieved by using a substrate temperature of 700 °C.

In summary, β-Ga_2O_3 thin films were grown on SCD (111) substrates at different substrate temperatures of 400, 500, 600, and 700 °C by RFMS technique. By using the substrate temperature of 700 °C, a monofamily $\{\bar{2}01\}$ crystal orientation of single-phase β-Ga_2O_3 thin films was obtained. By XRD PF study, two unique planes, including $(\bar{2}02)$ and (002), of $(\bar{2}01)$ β-Ga_2O_3 texture parallel to the (111) diamond texture with six different in-plane rotation domains were found. These two planes demonstrate a high $(\bar{2}01)$ orientation of the β-Ga_2O_3 thin film on diamond (111), with rotation occurring around the axis aligned with the $[\bar{2}01]$ direction. The two planes were also found when highly oriented β-Ga_2O_3 $(\bar{2}01)$ films were epitaxially grown on (110) a-plane sapphire substrate. This confirms that the β-Ga_2O_3 thin films with the $(\bar{2}01)$ preferred orientation were epitaxially grown not only in the perpendicular direction but also parallel to the diamond (111) substrate. Stranski–Krastanov (S–K) growth was a feasible dominant process in the epitaxial growth of β-Ga_2O_3 thin films on SCD (111) at 700 °C. The lattice mismatch of the epitaxial relationship along β-$Ga_2O_3(\bar{2}01) \parallel$ diamond(111) with β-$Ga_2O_3[010] \parallel$ diamond$[1\bar{2}1]$ was estimated to be −1.584% and 2.183%, respectively. Overall, the study demonstrated the successful heteroepitaxial growth of β-Ga_2O_3 thin films on SCD (111) substrates, providing valuable insights into the heteroepitaxial formation between β-Ga_2O_3 and diamond via sputtering and paving the way of further research on scalable β-Ga_2O_3/diamond heterostructures for future electronic and optoelectronic applications with not only high performance but also well self-thermal management.

Acknowledgments This work was partially supported by JSPS KAKENHI Grant No. 20K15044.

Authors' contributions

Kusaba and Sittimart contributed equally to this work.

ORCID iDs Phongsaphak Sittimart https://orcid.org/0000-0002-6035-1609
Yuki Katamune https://orcid.org/0000-0001-7527-3984
Taisuke Kageura https://orcid.org/0000-0002-9792-5223
Hiroshi Naragino https://orcid.org/0000-0002-3012-6603
Shinya Ohmagari https://orcid.org/0000-0001-5636-2316
Sreenath Mylo Valappil https://orcid.org/0000-0003-1225-5951
Abdelrahman Zkria https://orcid.org/0000-0003-0928-8752
Tsuyoshi Yoshitake https://orcid.org/0000-0002-5780-5585

---

1) M. Higashiwaki and G. H. Jessen, Appl. Phys. Lett. **112**, 060401 (2018).
2) M. Baldini, Z. Galazka, and G. Wagner, Mater. Sci. Semicond. Process. **78**, 132 (2018).
3) M. Higashiwaki, K. Sasaki, A. Kuramata, T. Masui, and S. Yamakoshi, Phys. Status Solidi Appl. Mater. Sci. **211**, 21 (2014).
4) J. Zhang et al., Nat. Commun. **13**, 3900 (2022).
5) P. Sittimart, S. Ohmagari, T. Matsumae, H. Umezawa, and T. Yoshitake, AIP Adv. **11**, 105114 (2021).
6) M. Malakoutian et al., Appl. Phys. Express **14**, 055502 (2021).
7) K. N. Heinselman, D. Haven, A. Zakutayev, and S. B. Reese, Cryst. Growth Des. **22**, 4854 (2022).
8) Z. Guo, A. Verma, X. Wu, F. Sun, A. Hickman, T. Masui, A. Kuramata, M. Higashiwaki, D. Jena, and T. Luo, Appl. Phys. Lett. **106**, 111909 (2015).
9) P. Sittimart, S. Ohmagari, and T. Yoshitake, Jpn. J. Appl. Phys. **60**, SBBD05 (2021).
10) T. Iwao, P. Sittimart, T. Yoshitake, H. Umezawa, and S. Ohmagari, Phys. Status Solidi **219**, 2100846 (2022).
11) P. Sittimart, S. Ohmagari, H. Umezawa, H. Kato, K. Ishiji, and T. Yoshitake, Adv. Opt. Mater. **11**, 2203006 (2023).
12) S. M. Valappil, S. Ohmagari, A. Zkria, P. Sittimart, E. Abubakr, H. Kato, and T. Yoshitake, AIP Adv. **12**, 085007 (2022).
13) T. Matsumae, Y. Kurashima, H. Umezawa, K. Tanaka, T. Ito, H. Watanabe, and H. Takagi, Appl. Phys. Lett. **116**, 141602 (2020).
14) H. Kim, S. Tarelkin, A. Polyakov, S. Troschiev, S. Nosukhin, M. Kuznetsov, and J. Kim, ECS J. Solid State Sci. Technol. **9**, 045004 (2020).
15) M. R. Karim, Z. Chen, Z. Feng, H.-L. Huang, J. M. Johnson, M. J. Tadjer, J. Hwang, and H. Zhao, J. Vac. Sci. Technol. A Vacuum, Surfaces, Film. **39**, 1965 (2021).
16) Y. C. Chen, Y. J. Lu, C. N. Lin, Y. Z. Tian, C. J. Gao, L. Dong, and C. X. Shan, J. Mater. Chem. C **6**, 5727 (2018).
17) T. Yoshitake, D. Nakagauchi, T. Ogawa, M. Itakura, N. Kuwano, Y. Tomokiyo, T. Kajiwara, and K. Nagayama, Appl. Phys. Lett. **86**, 262505 (2005).
18) A. K. Saikumar, S. D. Nehate, and K. B. Sundaram, ECS J. Solid State Sci. Technol. **8**, Q3064 (2019).
19) T. Yoshitake, Y. Inokuchi, A. Yuri, and K. Nagayama, Appl. Phys. Lett. **88**, 86 (2006).
20) J. C. Lavalley, M. Daturi, V. Montouillout, G. Clet, C. Otero Areán, M. Rodríguez Delgado, and A. Sahibed-dine, Phys. Chem. Chem. Phys. **5**, 1301 (2003).
21) L. M. Garten, A. Zakutayev, J. D. Perkins, B. P. Gorman, P. F. Ndione, and D. S. Ginley, MRS Commun. **6**, 348 (2016).

22) W. Seiler, M. Selmane, K. Abdelouhadi, and J. Perrière, Thin Solid Films **589**, 556 (2015).

23) S. Nakagomi and Y. Kokubun, J. Cryst. Growth **349**, 12 (2012).

24) B. Daudin, F. Widmann, G. Feuillet, Y. Samson, M. Arlery, and J. L. Rouvière, Phys. Rev. B **56**, R7069 (1997).

25) B. R. Tak, S. Dewan, A. Goyal, R. Pathak, V. Gupta, A. K. Kapoor, S. Nagarajan, and R. Singh, Appl. Surf. Sci. **465**, 973 (2019).

26) J. Wang, Y. Xiong, L. Ye, W. Li, G. Qin, H. Ruan, H. Zhang, L. Fang, C. Kong, and H. Li, Opt. Mater. (Amst). **112**, 110808 (2021).

27) C. Huang, W. Mu, H. Zhou, Y. Zhu, X. Xu, Z. Jia, L. Zheng, and X. Tao, RSC Adv. **8**, 6544 (2018).

28) M. Uddin Jewel, S. Hasan, and I. Ahmad, Comput. Mater. Sci. **218**, 111950 (2023).

29) J. M. Johnson et al., Phys. Rev. X **9**, 041027 (2019).